Virology 538 (2019) 24–34

Contents lists available at ScienceDirect

Virology

journal homepage: www.elsevier.com/locate/virology

Development of a novel screening platform for the identification of small molecule inhibitors of human adenovirus

Bratati Saha[a,b], Oliver Varette[b,c], William L. Stanford[a,d], Jean-Simon Diallo[b,c], Robin J. Parks[a,b,e,f,*]

[a] Regenerative Medicine Program, Ottawa Hospital Research Institute, Ottawa, Ontario, Canada
[b] Department of Biochemistry, Microbiology and Immunology, University of Ottawa, Ottawa, Ontario, Canada
[c] Cancer Therapeutics Program, Ottawa Hospital Research Institute, Ottawa, Ontario, Canada
[d] Department of Cellular and Molecular Medicine, University of Ottawa, Ottawa, Ontario, Canada
[e] Centre for Neuromuscular Disease, University of Ottawa, Ottawa, Ontario, Canada
[f] Department of Medicine, The Ottawa Hospital, Ottawa, Ontario, Canada

ARTICLE INFO

Keywords:
Adenovirus
Small-molecule screen
Antiviral
Cardiotonic steroids
Corticosteroids

ABSTRACT

Human adenovirus (HAdV) can cause severe disease and death in both immunocompromised and immunocompetent patients. The current standards of treatment are often ineffective, and no approved antiviral therapy against HAdV exists. We report here the design and validation of a fluorescence-based high-content screening platform for the identification of novel anti-HAdV compounds. The screen was conducted using a wildtype-like virus containing the red fluorescent protein (RFP) gene under the regulation of the HAdV major late promoter. Thus, RFP expression allows monitoring of viral late gene expression (a surrogate marker for virus replication), and compounds affecting virus growth can be easily discovered by quantifying RFP intensity. We used our platform to screen ~1200 FDA-approved small molecules, and identified several cardiotonic steroids, corticosteroids and chemotherapeutic agents as anti-HAdV compounds. Our screening platform provides the stringency necessary to detect compounds with varying degrees of antiviral activity, and facilitates drug discovery/repurposing to combat HAdV infections.

1. Introduction

The human adenovirus (HAdV) was first isolated in the 1950's from adenoid tissue (Hilleman and Werner, 1954; Rowe et al., 1953), and over 80 types (categorized into 7 species) have been identified to date (Binder et al., 2017; Dhingra et al., 2019). HAdV mainly causes minor illnesses in most individuals, and the type of disease and tissue tropism varies depending on the type involved. For example, HAdV species B and C are mainly responsible for respiratory infections, while species D is associated with conjunctivitis, and species F with the gastroenteritis (Lion, 2014). HAdV can also cause severe disease (including systemic infection and respiratory failure) and death in pediatric, geriatric, immunocompromised, and more rarely, in immunocompetent patients (Bhatti and Dhamoon, 2017; Binder et al., 2017; Kajon and Ison, 2016; Kojaoghlanian et al., 2003; Lion, 2014; Ying et al., 2014). In the clinic, antivirals typically used for other viral infections, such as cidofovir, ganciclovir and ribavirin, are used as standard treatments for HAdV-induced disease (Keyes et al., 2016; Lenaerts et al., 2008; Ronchi et al., 2014). However, these drugs often have low efficacy against HAdV and can have serious side effects such as nephrotoxicity (Caruso Brown et al., 2015; Keyes et al., 2016; Ronchi et al., 2014). Thus, a more effective anti-HAdV therapy is necessary. Brincidofovir, a phospholipid conjugate of cidofovir, recently received Fast Track designation from the FDA for treatment of HAdV infections (Detweiler et al., 2018; Ramsay et al., 2017), and clinical trials assessing virus-specific T-cells are currently ongoing (ClinicalTrials.gov; ClinicalTrials.gov). A live oral vaccine against types 4 and 7 was used by the U.S. military from 1971 to 1997, and then reintroduced in 2011 to limit HAdV infection in recruits (Binder et al., 2017). This vaccine is not available to the general population.

HAdV is a nuclear virus, with replication and progeny virion formation occurring within the nucleus of the infected cell (Berk, 2007). Proteins from the early viral transcription units (E1A, E1B, E2, E3 and E4) modulate cellular pathways to make the environment more conducive to viral gene expression and replication, or are necessary for the replication of the viral genome (Horwitz, 2004; King et al., 2018; Saha et al., 2014; Weitzman, 2005). In particular, the early region 1A (E1A) proteins are required for efficient virus replication as they transactivate expression of other HAdV genes, and the E2 proteins (DNA-binding

* Corresponding author. C4415 - 501 Smyth Road, Regenerative Medicine Program, Ottawa Hospital Research Institute, Ottawa, Ontario, K1H 8L6, Canada.
E-mail address: rparks@ohri.ca (R.J. Parks).

https://doi.org/10.1016/j.virol.2019.09.005
Received 26 June 2019; Received in revised form 7 September 2019; Accepted 12 September 2019
Available online 13 September 2019

protein or DBP, precursor terminal protein, viral DNA polymerase) are directly involved in synthesizing the viral DNA (de Jong et al., 2003; Flint, 1999; Frisch and Mymryk, 2002; Parker et al., 1998). The HAdV major late promoter (MLP) is only fully activated following initiation of viral genome replication, and it regulates expression of the late regions L1-L5 which mainly encode structural proteins (e.g. fiber, penton, hexon) (Ahi and Mittal, 2016; Wodrich et al., 2003; Young, 2003). As with all viruses, HAdV is reliant on the cellular machinery to assist in virus entry, viral gene expression, genome replication and production of progeny virions. For example, E1A interacts with a variety of cellular proteins, altering their regular functions and modifying the gene expression profile within the infected cell in order to provide an environment that promotes virus replication (Ferrari et al., 2008; Zhao et al., 2003). These cellular proteins include epigenetic modifiers, cell cycle regulators and transcription factors such as p300/CBP, p21, pRb, E2F1, TFIID and CtBP, amongst others (Horwitz et al., 2008; King et al., 2018). In addition to E1A, several other HAdV-encoded proteins (e.g. E1B, E3, E4, pVII) also alter host protein functions and gene expression throughout the virus lifecycle (Avgousti et al., 2017; Blackford and Grand, 2009; Horwitz, 2004; Weitzman, 2005). Small molecules that disrupt these interactions or pathways, without severely affecting cell health, may serve as effective anti-HAdV compounds. Indeed, changes in the localization of cellular RNA splicing proteins by cardiotonic steroids have been shown to alter HAdV-5 RNA processing, leading to drastic reductions in virus yield (Grosso et al., 2017). Tazarotene, a selective agonist of the retinoic acid receptor β, prevented virus replication in A549 cells (Wang et al., 2018). Identification of such compounds may eventually uncover effective therapeutic agents to treat HAdV-induced disease.

Screening of small molecules is a widely used, cost-effective drug-discovery approach which has led to the discovery of compounds against previously unexploited viral and host targets to combat a variety of viral infections (Johansen et al., 2013; Luthra et al., 2018; Nun et al., 2007; Stray et al., 2006). The majority of published studies on new HAdV inhibitors have evaluated only a small number of select compounds (Grosso et al., 2017; Marrugal-Lorenzo et al., 2018; Sanchez-Cespedes et al., 2016; Wang et al., 2018), and very few drug library screens have been performed (Duffy et al., 2013; Hartline et al., 2018). A fluorescence-based high throughput screen (HTS) was designed by Duffy et al. to specifically identify small molecules that inhibited coagulation factor X-mediated entry of HAdV-5 vectors by cells (Duffy et al., 2013). Another HTS conducted to discover novel HAdV inhibitors utilized E1-deficient, non-replicating viruses encoding GFP (under the control of the CMV promoter) to measure viral gene expression following infection and drug treatment (Sanchez-Cespedes et al., 2014). More recently, Hartline et al. described an approach using luminescence-based detection of drug-induced changes in viral cytopathic effects (CPE), which allowed broad-spectrum screening for antiviral compounds against various DNA viruses including HAdV (Hartline et al., 2018). Although the two latter studies identified several compounds with previously unreported anti-HAdV activity (FCV, 4-thio-IDU and a piperazine-2-one derivative), both screening systems relied on more indirect measurements of viral gene expression/replication, which may limit the ability of the screens to detect compounds with modest effects on virus replication.

To facilitate antiviral discovery and drug repurposing for ameliorating HAdV-induced disease, we designed an efficient high-content screening method using a wildtype-like HAdV-5 reporter construct, Ad-late/RFP. This virus contains the red fluorescent protein (RFP) gene under the regulation of the HAdV MLP and consequently, RFP expression is only detected upon full activation of the MLP following active viral DNA replication (Saha and Parks, 2019). As RFP levels reflect the degree of viral late gene expression and DNA replication (Saha and Parks, 2019), quantification of fluorescence intensity allows us to easily identify compounds that affect these processes. In this study, we have used our platform to screen ~1200 FDA-approved compounds. We validated the top positive hits by investigating their impact on cell health, viral gene expression, DNA replication and yield of infectious virions. We found that cardiotonic steroids suppressed multiple stages of the virus lifecycle and corticosteroids reduced early/late protein levels, resulting in decreased virus yield in both cases. Thus, our screening platform offers the sensitivity required to detect compounds that lead to even modest or transient reductions in viral gene expression/replication, as well as those with more robust antiviral activity.

2. Materials and methods

2.1. Cell lines and reagents

Most experiments were conducted in the human lung adenocarcinoma-derived A549 cell line (CCL-185, ATCC), unless otherwise indicated. To monitor significant changes in cell viability and density in the small molecule screen and dose-response assays, A549 cells were transduced with a lentiviral vector to constitutively express green fluorescent protein (GFP) (Wong et al., 2016). The A549-GFP cell line grows and supports HAdV replication as well as the parental A549 cell line, and has been referred to as “GFP-expressing A549 cells” where applicable in this study. Both cell lines were cultured in Minimum Essential Medium (MEM, Sigma-Aldrich) containing 10% (v/v) Fetal Bovine Serum (FBS, Sigma Aldrich), 2 mM GlutaMAX (Invitrogen) and 1x antibiotic-antimycotic (Invitrogen). MRC-5 cells (CCL-171, ATCC) were cultured similarly in Dulbecco's Modified Eagle Medium (DMEM, Sigma-Aldrich).

The Prestwick Chemical Library was obtained from Prestwick Chemical. For validation and follow-up experiments, SAHA (SML0061; ≥98% purity by HPLC), digoxin (D6003; ≥95%) and lanatoside C (L2261; ≥95%) were purchased from Sigma; cytarabine (16069; ≥95%), methotrexate (13960; ≥98%) and digitoxigenin (18229; ≥98%) were purchased from Cayman Chemical; dexamethasone acetate (SC-204714; ≥99%) and flunisolide (SC-215039; ≥98%) were purchased from Santa Cruz Biotechnology. All compounds were dissolved in DMSO to prepare stock solutions and diluted in cell media for treatments.

2.2. HAdV constructs

Construction of the Ad-late/RFP has been described in detail previously (Saha and Parks, 2019). Briefly, the monomeric RFP coding sequence with an upstream splice acceptor site replaces the viral E3 region, which places RFP expression under the control of the viral MLP (Tollefson et al., 1996). This construct was generated based on HAdV-5, using a combination of conventional cloning and bacterial recombination (Chartier et al., 1996). The virus was propagated in 293 cells and purified by cesium chloride buoyant density centrifugation using standard procedures (Ross and Parks, 2009). Viral titer (plaque forming units) was determined by plaque assay on 293 cells as previously reported (Saha and Parks, 2017).

2.3. Infection and drug treatment

Unless otherwise indicated, medium was removed from confluent monolayers of A549 cells before infecting with the Ad-late/RFP. Multiplicity of infection (MOI) was calculated as plaque-forming units (PFU) per cell. Virus inoculums were diluted in phosphate-buffered saline (PBS, Sigma-Aldrich) and added to the cells for 1 h at 37°C with periodic rocking. Medium containing either vehicle or drug was then added to the cells, followed by incubation in a humidified CO_2 incubator at 37°C until the indicated time points.

For experiments involving pretreatment with compounds, the cells were incubated with vehicle/drug-containing medium for 2 h at 37°C before infection. Drug treatment was maintained throughout the course of infection and the treatment medium was replaced every 24 h for experiments that extended beyond one day.

2.4. Fluorescence microscopy

Live cells were imaged 18–24 h after infection using a 10x objective

on a Zeiss Axio Observer.Z1 microscope equipped with an Axiocam MRC camera and ZEN 2 software for image processing.

2.5. Immunoblot analysis

Cells were lysed in 2x Laemmli buffer containing 5% β-mercaptoethanol, subjected to SDS-PAGE and transferred to a polyvinylidene difluoride (PVDF) membrane (Millipore) as previously described (Saha and Parks, 2017). The membrane was blocked with 5% milk in tris-buffered saline containing 0.2% Tween 20 (Thermo Fisher Scientific), and probed with antibodies diluted in the 5% milk solution. The following primary antibodies were used: HAdV-5 fiber (1/10,000 dilution; MS-1027-P0, Neomarkers), HAdV-5 E1A (1/5,000; MA5-13643, Invitrogen), vinculin (1/10,000; ab129002, Abcam), tubulin (1/5,000; CP06, Calbiochem), actin (1/10,000; A1978, Sigma Aldrich), and RFP (1/5,000; ab62341, Abcam). The HAdV-5 fiber antibody from Neomarkers was discontinued during the course of this study. Therefore, hexon was detected instead using the HAdV-5 antibody from Abcam (1/10,000; ab6982) to examine late gene expression in some of the immunoblots. This antibody detects all of the major HAdV-5 structural proteins, and also cross-reacts with some of the HAdV-4 and HAdV-7 capsid proteins. The monoclonal antibody against HAdV-5 DBP (antibody 72K–B6, 1/5,000 dilution) was a kind gift from Dr. Arnold Levine (Institute for Advanced Study, Princeton, New Jersey) (Reich et al., 1983). The membranes were then washed three times in TBST and incubated with the appropriate secondary antibodies conjugated to horseradish peroxidase (HRP). Blots were developed using the Immobilon Classico Western HRP Substrate (Millipore). All immunoblot data are representative of two or more independent experiments.

2.6. Small molecule screen and RFP quantification assays

GFP-expressing A549 cells were seeded in 96-well plates at a density of 20,000 cells/well using the MicroFlo Select Dispenser (BioTek). Compounds from the library plates were diluted to a working concentration in PBS containing 10% DMSO, and vehicle/compounds were added to confluent monolayers of cells for pretreatment (final concentration of 250 nM in culture media) using the Precision Microplate Pipetting System (BioTek). After 2 h of pretreatment, these cells were infected with Ad-late/RFP (MOI 10) in the presence of the compounds. At 24 hpi, the cell media was aspirated and the cell monolayers were washed once in PBS. The cells were fixed with freshly made 4% w/v paraformaldehyde (pH 7) for 15 min. The fixed cells were stored in PBS overnight at 4°C. The following day, the PBS was removed and the cell nuclei were stained for 15–20 min with 10 μg/ml Hoechst 33342 (Life Technologies) diluted in PBS. New PBS was placed back on the stained cells before RFP quantification using the Cellomics High Content Screening (HCS) Platform and the Cellomics navigator version of the HCS Studio software (Thermo Fisher Scientific). The 10x objective and the following filters were used: $386_{\text{excitation (ex)}}$ nm for Hoechst, 549_{ex} nm for RFP and 485_{ex} nm for GFP. Roughly 1,000 cells (Hoechst-stained intact nuclei) were analyzed per well and their total RFP intensity was measured. Since each library plate was treated and screened in triplicate, the mean data from the three replicate plates was used for analysis. The mean RFP intensities in drug-treated wells were calculated as a percentage of the mean intensities in vehicle-treated wells. Further information on screen parameters and analysis is available upon request.

For the dose-response assays, drug treatment, infection, cell fixation and RFP quantification were carried out as described above for the screen.

2.7. Quantitative real-time PCR (qPCR)

A549 cells were pretreated with compounds and infected as described above. Medium was removed from the infected cells at the indicated time points and the cells were incubated overnight in SDS-proteinase K buffer (10 mM Tris-HCl pH 7.4, 10 mM EDTA, 1% w/v SDS, 1 mg/ml proteinase K) at 37°C. DNA was extracted from the cell lysates using the standard phenol-chloroform method, precipitated with ethanol and NaCl, and the resulting DNA pellet was dissolved in 1x Tris-EDTA (TE) buffer. qPCR was conducted as previously described (Ross et al., 2011) using 200 ng of genomic DNA per reaction. The following primers were used: 5′-CTT ACC CCC AAC GAG TTT GA and 5′-GGA GTA CAT GCG GTC CTT GT for HAdV hexon; 5′-CCA TTA AAC CAG TTG CCG TGA GAG and 5′-GGC GTT TAC AGC TCA AGT CCA AAG for HAdV E1A. Viral genome copy numbers were calculated from the Ct values using a standard curve obtained using serial dilutions of the pRP3089, the bacterial plasmid used to generate Ad-late/RFP.

2.8. RNA extraction and reverse transcription qPCR

A549 cells were pretreated with compounds and infected as described above. Medium was removed from the infected cells and total cellular RNA was extracted using TRIzol Reagent (Thermo Fisher Scientific) and the PureLink RNA Mini Kit (Ambion) according to the manufacturer's protocol. To synthesize cDNA from the extracted RNA by reverse transcription (RT), the M-MuLV Reverse Transcriptase was used (New England Biolabs) along with a mixture of random hexamers (New England Biolabs), according to the manufacturer's protocol. 800 ng of RNA was used per RT reaction. qPCR was then conducted as described above using 2 μl of the cDNA mixture.

2.9. Plaque assay for virus yield

Monolayers of A549 cells were pretreated with each compound, and infected with Ad-late/RFP (MOI 10). The virus inoculum was removed after 1 h of infection, the cells were washed with PBS, and fresh medium containing vehicle or compounds was added. After 24 h of infection, the cells were collected by scraping into the medium, 40% w/v sucrose (diluted in 10 mM Tris) was added to a final concentration of 4% v/v, and the samples were flash-frozen in ethanol and dry ice. For the plaque assay, monolayers of A549 cells were infected with dilutions of this cell lysate. After 1 h of infection, the cells were overlaid with medium containing agarose (50% v/v of a 1% w/v agarose solution, 43% clear 2x MEM, 5% FBS, 1% GlutaMAX and 1% antibiotic-antimycotic) and placed in a 37°C incubator. Plaques were counted 8–10 days later.

2.10. MTS metabolic activity assays

96-well plates of A549 cells were pretreated with compounds and infected with Ad-late/RFP (MOI 10). 24 h post infection, the metabolic activity was determined using the CellTiter 96 AQueous Non-Radioactive Cell Proliferation Assay (Promega) according to the manufacturer's instructions. Briefly, cells were incubated for 1 h at 37°C with 20 μl of the MTS substrate, and absorbance readings were obtained at 490 nm using the SpectraMax 190 plate spectrophotometer (Molecular Devices).

3. Results

3.1. Design and optimization of the small molecule screen

We generated a replication-competent ($E1^+$), wildtype-like HAdV construct, designated Ad-late/RFP, which encodes the RFP gene under the regulation of the viral MLP (Saha and Parks, 2019). Since the MLP is only fully active following viral DNA replication (Thomas and Mathews, 1980; Tollefson et al., 1996), RFP expression from Ad-late/RFP increases with time during late infection (Fig. 1A). In a previous study, we confirmed that Ad-late/RFP grows similar to the wildtype HAdV-5 in terms of protein expression and DNA replication, and that RFP is produced only when virus replication occurs (Saha and Parks, 2019). Thus, RFP fluorescence can be used as a surrogate marker to efficiently monitor any changes in HAdV DNA and late protein levels induced by small molecules that affect the earlier stages of the virus lifecycle, or the stability of viral RNA/proteins.

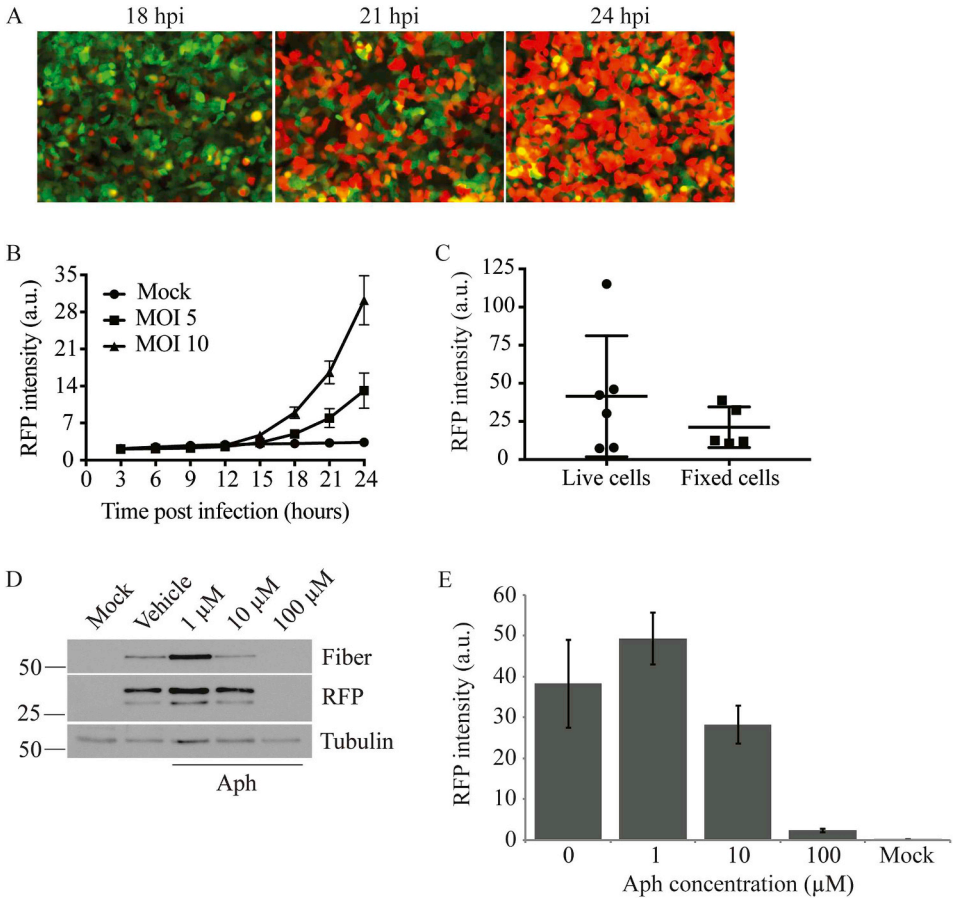

Fig. 1. Optimization and validation of a small molecule screen for anti-HAdV compounds. GFP-expressing A549 cells were infected with Ad-late/RFP at an MOI of 10, unless indicated otherwise. (A) Infected, live cells were visualized after the onset of viral DNA replication, at the indicated times post infection. RFP expression from Ad-late/RFP increases along with virus replication over time. (B) RFP intensities within infected cells (MOI 5 or 10 of Ad-late/RFP) were quantified every 3 h over 24 h post infection (hpi) in live cells using the Cellomics ArrayScan VTI High Content Screening Platform. a.u. represents arbitrary units. Error bars represent standard deviation (SD) of analytical replicates (n = 14). (C) RFP fluorescence in live or fixed cells was quantified as in panel B. Intensities were less variable between five independent experiments in the fixed-cell screen. Error bars represent SD of experimental replicates (n = 5 or 6). (D) Infected cells were treated with vehicle or 1–100 μM aphidicolin (Aph). Cell lysates were collected at 24 h after infection and drug treatment for analysis of viral late gene expression by immunoblot. Aph decreases fiber and RFP production in a dose-dependent manner. (E) Infected, Aph-treated cells were fixed at 24 hpi and the RFP intensity was quantified as in panel B. The results corroborate observations from the immunoblot. Error bars represent SD of analytical replicates (n = 16).

To detect real-time changes in RFP intensity induced by small molecules during a screen, we first attempted to measure the intensities over a time course of infection in live (i.e. non-fixed) GFP-expressing A549 cells. We designed a live-cell screen protocol using the Ad-late/RFP and the Cellomics ArrayScan VTI HCS Platform connected to a Live Cell Module, which controls temperature and CO_2 in the imaging chamber. Infected cells were placed in the Live Cell Chamber over a 24-h time course of infection to periodically quantify RFP fluorescence. RFP increased 10- to 30-fold over time and as expected, the extent of increase positively correlated with the MOI of virus (Fig. 1B). However, with the live-cell imaging approach, high variability was observed within experimental replicates at each time point (the 24 h time points with Ad-late/RFP at MOI 10 are shown in Fig. 1B; mean of 42 ± 40 a.u.). Furthermore, in many of the preliminary test experiments we conducted with live-cell imaging (similar to that in Fig. 1B), the virus simply failed to propagate, perhaps due to the non-optimal cell growth conditions within the Live Cell Chamber (as explained in the Discussion section below). This issue was resolved and the experimental variability was significantly reduced (22 ± 13 a.u.) when RFP intensity was quantified following cell fixation at 24 hpi (Fig. 1C). As such, all subsequent RFP quantification assays and the screen were conducted on drug-treated and infected GFP-expressing cells that were fixed at 24 hpi as described in the Materials and Methods.

To test the reliability of the fixed-cell screen protocol, we conducted a dose-response assay with aphidicolin (Aph), a DNA polymerase inhibitor that prevents HAdV replication by interfering with dCTP incorporation during DNA synthesis (Krokan et al., 1981). Immunoblot analysis of Ad-late/RFP-infected, Aph-treated cells showed that the drug reduced protein levels of both fiber and RFP in a dose-dependent manner (Fig. 1D). These results were corroborated by the RFP intensities quantified using the Cellomics ArrayScan in infected, drug-treated cells at 24 hpi (Fig. 1E), which confirmed the reliability of the screen protocol.

3.2. Identification and validation of HAdV inhibitors from the Prestwick Chemical Library

We next used our platform to screen ~1200 chemically and pharmacologically diverse compounds in the Prestwick Chemical Library to identify novel compounds with anti-HAdV activity. Although the screened compounds are likely optimally active at different concentrations *in vivo*, we used a single concentration in our initial pilot screen and subsequently tested the positive hits at varying concentrations in our validation experiments. In a recent study, we showed that the pan-histone deacetylase (HDAC) inhibitor SAHA reduces RFP expression from Ad-late/RFP, as well as virus yield, in a dose-dependent manner (Saha and Parks, 2019). SAHA induced more than a 50% decrease in RFP intensity at a concentration of 250 nM. Thus, SAHA was used as a positive control for reduction of RFP levels, while vehicle treatment served as the negative control, on each screen plate of 80 test compounds from the library (Fig. 2A). We also selected 250 nM as the screen concentration because it is relatively low and would allow detection of compounds with higher efficacy against Ad-late/RFP. Each library plate was screened in triplicate, and the mean data for one representative plate is shown in Fig. 2B. While the majority of the small molecules screened did not affect RFP compared to vehicle treatment, we identified a subset of compounds that either decreased or increased RFP intensities significantly (Fig. 2C–D). To limit the number of compounds considered for further investigation, we selected fourteen that decreased RFP by at least 50% (Fig. 2D) and conducted subsequent dose-response assays to confirm the positive hits (data not shown). Of those, eleven compounds were confirmed to indeed reduce RFP from Ad-late/RFP at nanomolar concentrations (Table 1).

The most effective inhibitors of RFP expression identified from the screen were digoxin, digitoxigenin and lanatoside C (Table 1). The anti-HAdV activity of cardiotonic steroids was recently reported in another

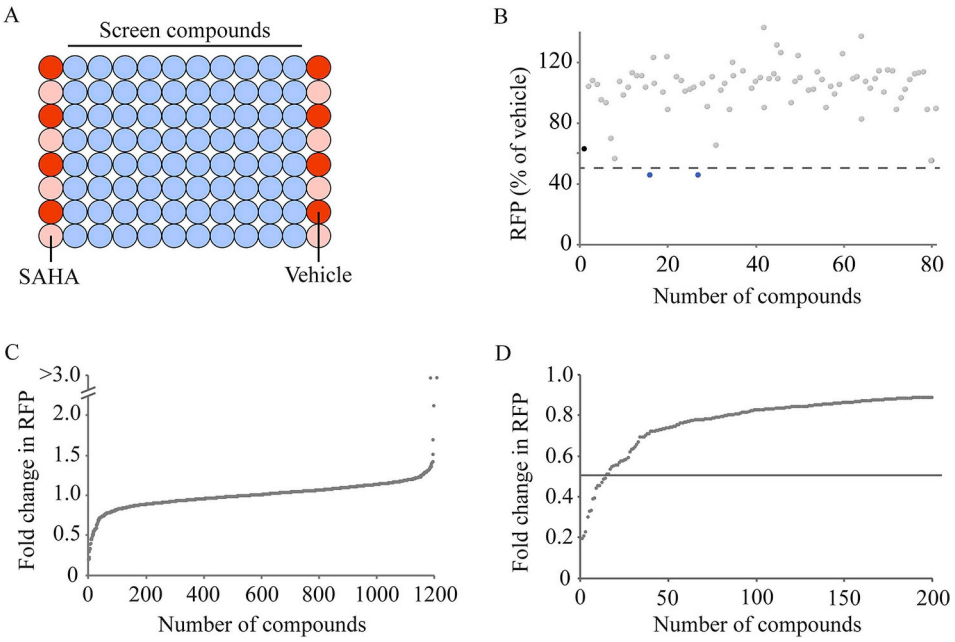

Fig. 2. Screen of the Prestwick Chemical Library. (A) Layout of 96-well plates in the screen. Test compounds were added to 80 wells (blue). Vehicle (negative control) and SAHA (positive control) were added in alternate wells of the first and last columns. Cells were pretreated with vehicle or compounds at a concentration of 0.25 μM for 2 h prior to infection with Ad-late/RFP (MOI 10). Cells were fixed at 24 hpi and RFP intensities were measured using the Cellomics ArrayScan. (B) Representative data from a single screen plate (80 test compounds). Changes in RFP levels were calculated as a percentage of vehicle treatment. The black data point represents SAHA, while the blue data points represent the compounds that reduced RFP expression by more than 50%. Each set of compounds was screened in three independent assays and the data points represent the mean. (C) The average RFP intensities in drug-treated cells were calculated as fold change relative to vehicle-treated cells. Fold changes for all 1200 compounds were plotted in order of increasing magnitude. While most compounds did not alter RFP expression from Ad-late/RFP, several compounds were found to either significantly reduce or moderately enhance RFP levels. (D) A magnified view of panel C highlighting fourteen compounds that reduced RFP intensities to half that in vehicle-treated cells. Error bars have been omitted for clarity.

Table 1
Validated positive hits from the Prestwick Chemical Library. Of the fourteen compounds that reduced RFP levels by at least 50% in the initial screen, eleven were confirmed to decrease RFP from the Ad-late/RFP in subsequent assays. The percentage values indicate the RFP intensity in cells treated with 0.25 μM drug relative to vehicle-treated cells (100% RFP) in the screen.

Cardenolides	Corticosteroids	Others
(1) Lanatoside C (19%)	(4) Dexamethasone acetate (39%)	(9) Cytarabine (30%)
(2) Digoxin (21%)	(5) Flumethasone (46%)	(10) Methotrexate (33%)
(3) Digitoxigenin (23%)	(6) Flurandrenolide (47%)	(11) Podophyllotoxin (45%)
	(7) Diflorasone diacetate (49%)	
	(8) Flunisolide (49%)	

study (Grosso et al., 2017), which further supports the reliability of our screen results. To validate these compounds in our system, we first conducted a dose-response assay to determine whether these compounds were effective in reducing RFP intensities at low concentrations. As in the screen, GFP-expressing A549 cells were pretreated with the compounds (~15 nM–1 μM), and infected for 24 h prior to RFP quantification in fixed cells. All three compounds were more effective than SAHA in decreasing RFP at the concentrations tested (Fig. 3A). The IC_{50} values (with regards to RFP levels) were determined to be approximately 240 nM, 20 nM, 64 nM and 32 nM for SAHA, digoxin, digitoxigenin and lanatoside C, respectively. This inhibitory effect on RFP was not due to compromised cell health as metabolic activity was 80% or above for all three compounds compared to vehicle, at least at concentrations up to ~100 nM (Fig. 3B), and endogenous GFP fluorescence from these cells was not reduced (data not shown). Our results are consistent with the findings of Grosso et al., who also found that cardiotonic steroids suppress HAdV replication, but not cell viability, at similar concentrations (Grosso et al., 2017).

We next conducted dose-response and MTS assays with three additional compounds which were selected based on their effectiveness (Table 1): chemotherapy agents cytarabine and methotrexate, and the anti-inflammatory corticosteroid dexamethasone. We included flunisolide for validation as it is also a corticosteroid, and would be expected to have similar efficacy as dexamethasone. These two classes of drugs target different cellular proteins and pathways than the cardiotonic steroids, and likely inhibit Ad-late/RFP gene expression by other mechanisms. Both cytarabine and methotrexate significantly reduced RFP fluorescence at low concentrations, while the corticosteroids reduced RFP to 30–40% of vehicle treatment at all concentrations examined (Fig. 3C). With the exception of methotrexate, these compounds also did not affect cellular metabolic activity or GFP intensity (Fig. 3D and data not shown). The effect of methotrexate on RFP may be (at least partially) due to drug-induced cytotoxicity, and it was excluded from further investigation. Overall, these results suggest that the screening platform we developed provides the sensitivity and stringency necessary to detect and quantify varying degrees of small molecule-induced changes on HAdV gene expression.

3.3. Cardiotonic steroids are potent inhibitors of HAdV

Since digoxin, digitoxigenin and lanatoside C were very effective in reducing RFP levels at low concentrations in the validation assays (Fig. 3), we conducted further studies to determine whether other stages of the virus lifecycle are impacted by these drugs (e.g. early/late gene transcription, protein expression, DNA replication). Cells were pretreated with vehicle or each compound at 100 nM for 2 h, and infected with Ad-late/RFP in the presence of the compounds. Although analysis of E1A transcript levels at 6 hpi showed no difference between vehicle- and drug-treated cells (Fig. 4A), early proteins E1A and DBP were both decreased substantially at 8 hpi (Fig. 4B). E1A transcript levels also remained unchanged between the various treatments at 24 hpi (Fig. 4A). E1A and DBP proteins were easily detected at this later time point, but the overall amount was reduced relative to vehicle-

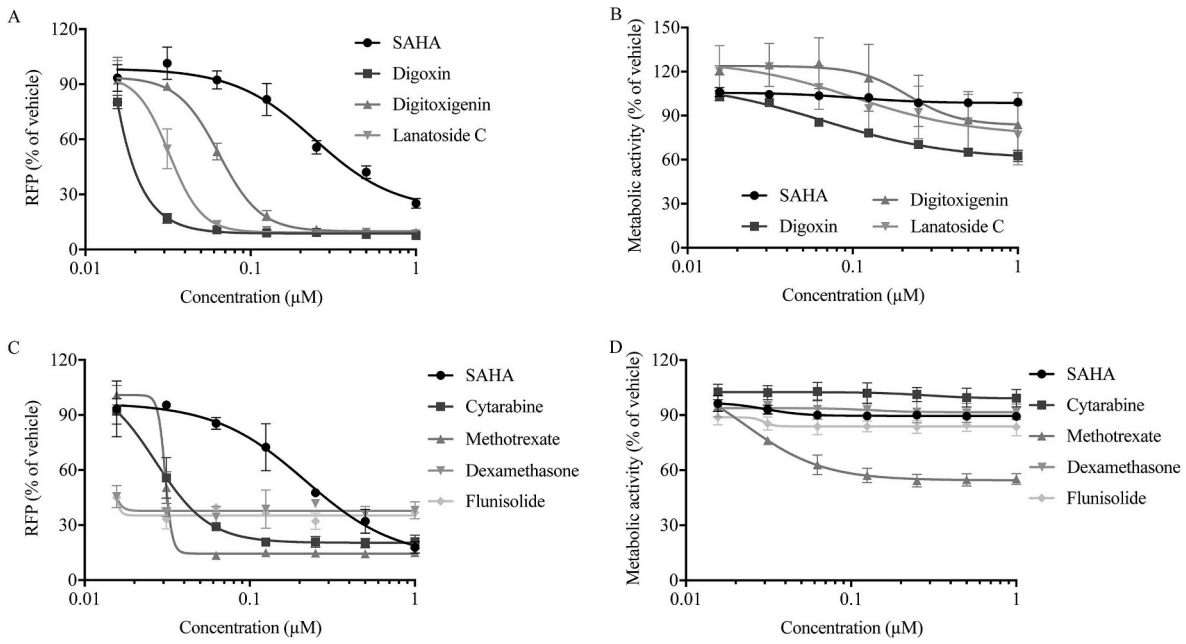

Fig. 3. Dose-dependent effects of the selected positive hits on RFP and cellular metabolic activity. GFP-expressing A549 cells were treated for 2 h with each compound at the indicated concentrations, then infected with Ad-late/RFP (MOI 10) for 24 h. (A, C) Infected, drug-treated cells were fixed and RFP intensities were quantified using the Cellomics ArrayScan. (B, D) Cellular metabolic activity was determined by MTS assay. Both RFP expression and metabolic activity were calculated as a percentage of vehicle treatment, and the data was fitted to a sigmoidal or dose-response curve in GraphPad Prism. Error bars represent SD of experimental replicates (n = 3).

treated cells (Fig. 4B). These observations suggest that the cardiotonic steroids do not affect E1A transcription or mRNA stability, but may affect E1A protein levels by altering protein translation or stability.

In the HAdV lifecycle, early gene expression is followed by viral DNA replication. Therefore, we next examined viral genome copy numbers at early and late times of infection in cells treated with the cardiotonic steroids. qPCR with primers specific to the viral hexon region showed that the Ad-late/RFP genome copy numbers at 8 hpi (before the onset of viral DNA replication) were similar in vehicle- and drug-treated cells (Fig. 4C), suggesting that virus entry was not affected. Digoxin was a potent inhibitor of Ad-late/RFP DNA replication as it led to a 1,000-fold decrease in Ad-late/RFP genome copy numbers at 24 hpi, and a continued trend towards decreased genome copies was observed at 48 hpi (Fig. 4C). Although less effective than digoxin, reduced DNA replication was also evident at 24 hpi with digitoxigenin and lanatoside C, but there were no significant differences with these compounds later on (Fig. 4C). This is unlikely due to drug degradation over the time course of infection as all three compounds have fairly long half-lives (at least 30 h *in vivo*) (Doherty and Kane, 1973), and the cell medium containing drug was replaced every 24 h in our experiments. As expected, all three compounds affected late gene transcription at 24 hpi (Fig. 4D), which was concomitant with a substantial decrease in viral late proteins (fiber, hexon, penton) and RFP levels (Fig. 4E). Late protein expression remained low with digoxin and lanatoside C at 48 hpi (Fig. 4E), but late transcript levels were comparable to vehicle treatment at that time point (Fig. 4D), further supporting the possibility that these compounds may act by altering protein production and/or stability. Inhibition of multiple stages of the HAdV lifecycle by the cardiotonic steroids consequently led to a 100- to 1000-fold reduction in Ad-late/RFP yield as determined by plaque assay of virus recovered from treated cells (Fig. 4F). The antiviral activity of the cardiotonic steroids was also observed against Ad-late/RFP in primary MRC-5 cells (Fig. 4G and S1A), and against clinically relevant types 4 and 7 (Fig. 4H and S1B). Our results, combined with that obtained by Grosso et al. (2017), confirm that cardiotonic steroids are effective inhibitors of HAdV, and these compounds were successfully detected by our screening method.

3.4. Cytarabine, dexamethasone and flunisolide have modest anti-HAdV activity

We next examined how cytarabine, dexamethasone and flunisolide affect the HAdV lifecycle. Each compound was used at 200 nM, and drug treatment and infection were carried out as described above for the cardiotonic steroids. Interestingly, cytarabine did not decrease the transcript levels of E1A or expression of the early genes (Fig. 5A and B). Although a trend towards reduced E1A transcript was observed with dexamethasone and flunisolide at 6 hpi, this was not statistically significant (Fig. 5A). However, both E1A and DBP expression was reduced at 8 hpi (Fig. 5B). By 24 hpi, transcript levels of E1A were all comparable to vehicle treatment (Fig. 5A), and a small decrease in E1A protein was still evident with the corticosteroids (Fig. 5B). Somewhat surprisingly, we did not detect any differences in Ad-late/RFP genome copy numbers with any of the compounds, at least at the time points examined (Fig. 5C). This observation may mimic our results with SAHA, where inhibition of viral DNA replication was greater earlier on during the replicative phase of infection, and was not as pronounced at later time points (Saha and Parks, 2019). Alternatively, early proteins may increase over time to sufficient amounts that permit nearly normal levels of DNA replication in late infection.

As with early transcripts, there were no significant changes in late transcript levels with cytarabine and the corticosteroids, but we did detect a decrease in late proteins at 24 hpi (Fig. 5E). For all three compounds, the extent of late protein reduction was more pronounced at lower MOIs (Fig. 5F, S2A and S2B) which are more relevant to clinical settings. Treatment with cytarabine and the corticosteroids also reduced virus yield (~3- to ~30-fold) from infected cells (Fig. 5G). Thus, these compounds all act as antivirals mainly through effects on HAdV protein expression, ultimately lowering virus yield. In MRC-5 cells, cytarabine reduced hexon expression to a similar extent as in A549s (Fig. 5H), but the corticosteroids were ineffective (data not shown). Taken together, our results illustrate that the screening method we developed provides the necessary sensitivity to detect even modest or transient changes in viral gene expression, which can impact upon virus growth.

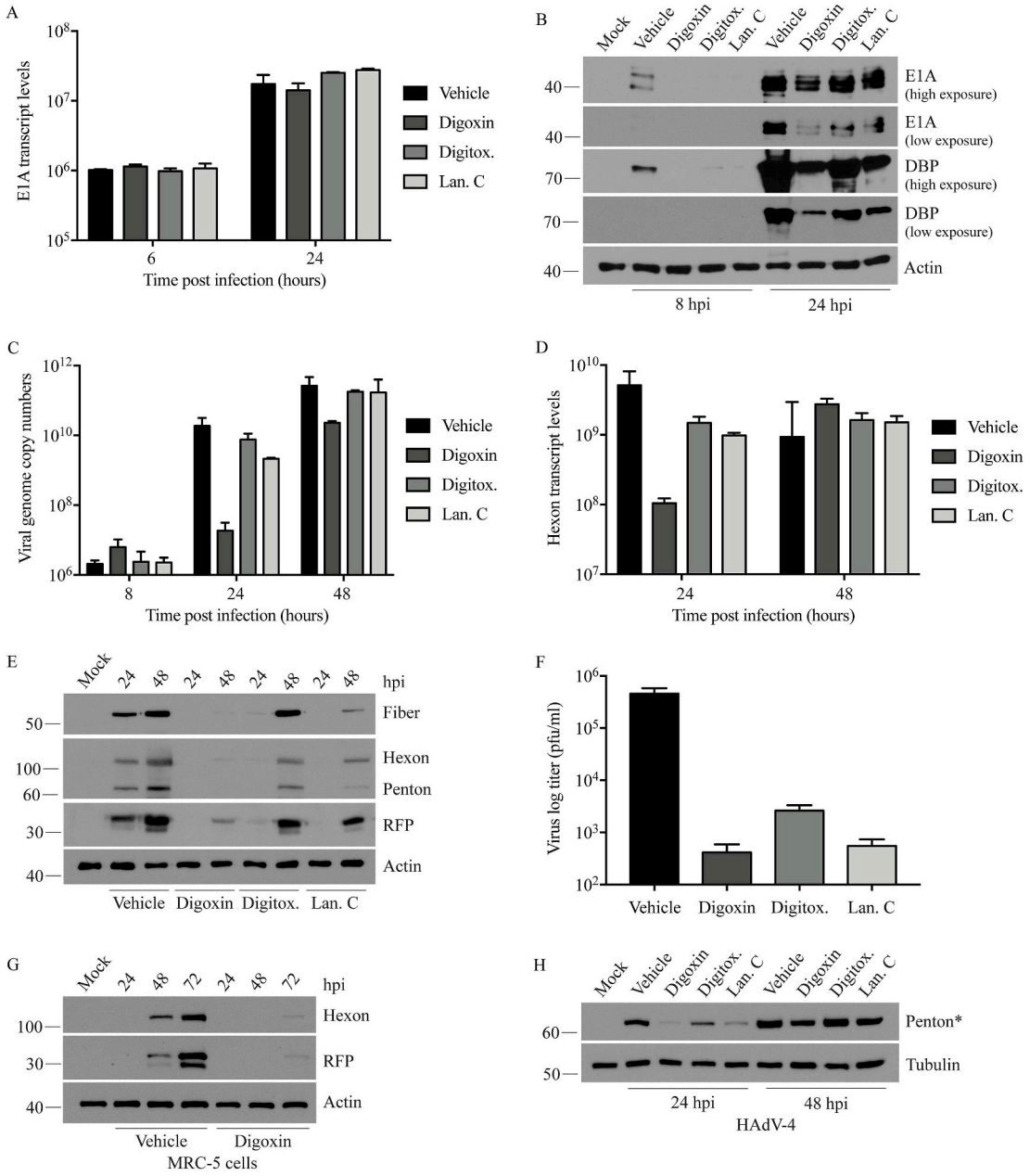

Fig. 4. Cardiotonic steroids reduce virus gene expression, DNA replication and yield. In all experiments, cells were pretreated with vehicle, digoxin, digitoxigenin or lanatoside C at 100 nM for 2 h. Treated cells were infected at an MOI of 10 in the presence of the compounds, and cell lysates were collected at the indicated times for analysis of viral proteins/DNA/RNA. (A, D) Total RNA was extracted from Ad-late/RFP-infected A549 cells and cDNA was generated by reverse transcription. qPCR analysis was conducted using primers binding to the HAdV E1A (A) or hexon (D) regions. (B, E) A549 cell lysates were subjected to immunoblot analysis for detection of early (E1A, DBP) and late (fiber, RFP) proteins from Ad-late/RFP. (C) Genomic DNA (gDNA) was extracted from infected A549 cells at the indicated times for qPCR using primers specific to the hexon gene. Ad-late/RFP genome copy numbers per 200 ng of total gDNA are reported. (F) Drug-treated A549 cells were infected with Ad-late/RFP and collected at 24 hpi to determine virus yield by plaque assay. (G) Pretreated MRC-5 cells were infected with Ad-late/RFP and cell lysates were collected for immunoblotting. (H) A549 cells were pre-treated with vehicle or compounds, and infected with HAdV-4. *The protein (detected using an anti-HAdV-5 antibody that cross-reacts with some of the HAdV-4 and HAdV-7 capsid proteins) is most likely penton based on its size of ~60 kDa. Error bars represent SD (n = 2 for panels A and D; n = 3 for panels C and F).

4. Discussion and conclusions

Development of various high-throughput screening platforms have allowed the identification of novel antiviral compounds, and highlighted the potential of repurposing existing drugs as antivirals for several viruses including Ebola, hepatitis B virus and herpes simplex virus (de Wispelaere et al., 2017; Johansen et al., 2013; Luthra et al., 2018; Nun et al., 2007; Pilger et al., 2004; Stray et al., 2006). To identify novel small molecule inhibitors of HAdV, we developed an efficient screening platform using a HAdV reporter construct, designated Ad-late/RFP (Saha and Parks, 2019), which encodes the RFP gene under regulation of the viral MLP. As such, RFP expression coincides with the expression of the endogenous viral late genes and reflects the extent of DNA replication (Saha and Parks, 2019). Thus, virus replication can be monitored by RFP fluorescence (Fig. 1), which is sufficiently sensitive to detect small changes in virus growth. Although this virus can be used for both live-cell and fixed-cell imaging, we observed higher experimental variability in preliminary screens using live-cell imaging (Fig. 1). Cell fixation reduced this variability (Fig. 1), and overcame several other drawbacks associated with screening live cells, including (i) impacts of temperature and CO_2

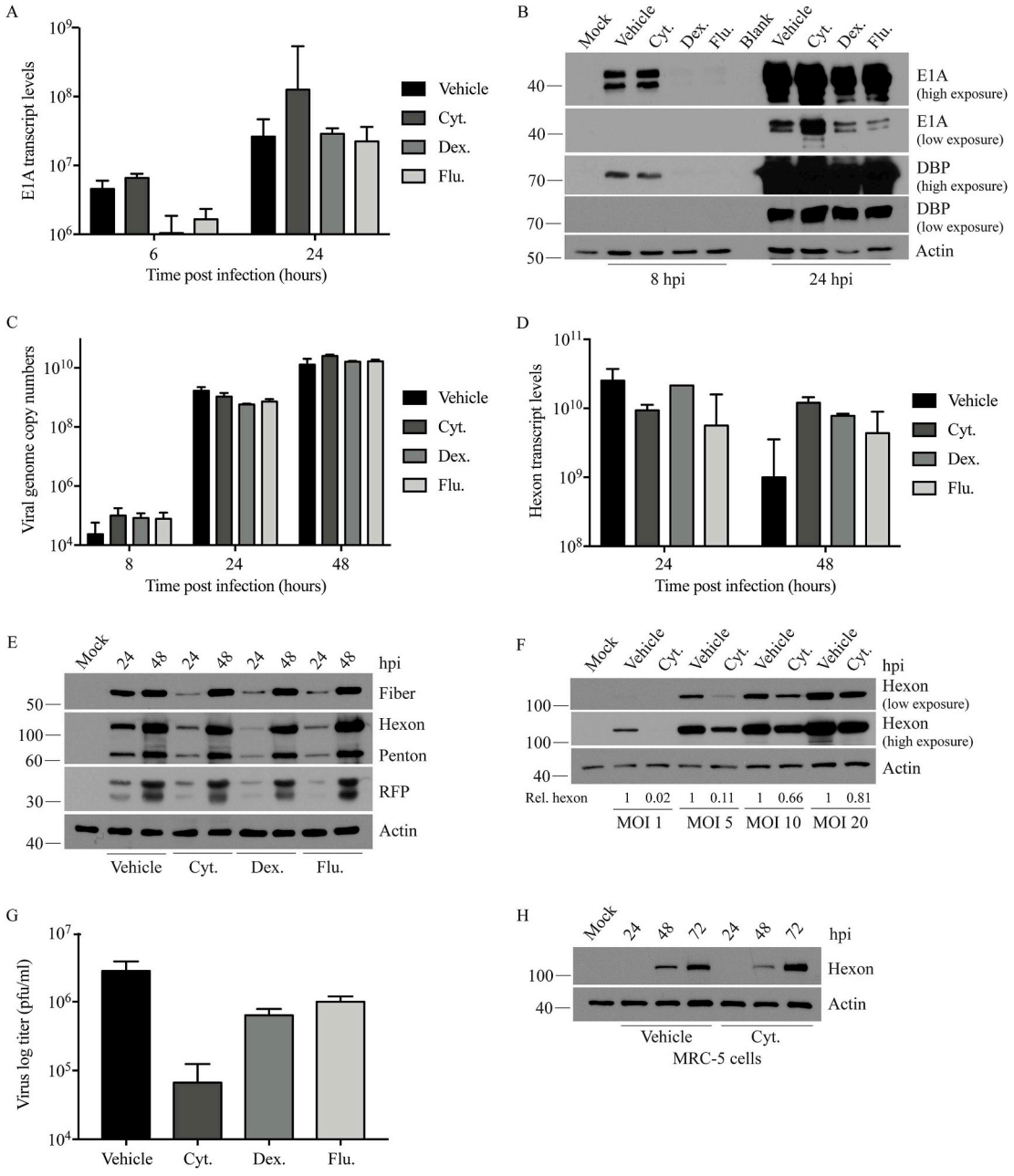

Fig. 5. Cytarabine, dexamethasone and flunisolide reduce HAdV gene expression and yield. All cells were pretreated with vehicle, cytarabine, dexamethasone or flunisolide at 200 nM for 2 h, and then infected with Ad-late/RFP (MOI 10, unless otherwise indicated) over the indicated time periods. (A, D) RNA was extracted from infected A549 cells and reverse transcribed to cDNA. qPCR analysis was conducted using primers to the HAdV E1A (A) or hexon (D) coding regions. (B, E) A549 cell lysates were examined for viral early (B) and late (E) protein expression by immunoblot. (C) gDNA was extracted from infected A549 cells at the indicated times for qPCR using primers specific to hexon. Viral genome copy numbers per 200 ng of total gDNA are reported. (F) Following pretreatment, A549 cells were infected at various MOIs for 24 h, and crude protein extracts from the cells were used for immunoblot analysis. Relative hexon protein levels were determined using the Image J software. Hexon bands were first normalized to actin (loading control), followed by calculation of drug-treated band intensities relative to vehicle-treated bands at each specific MOI. (G) Infected, drug-treated A549 cells were collected at 24 hpi and subjected to plaque assay for quantification of virus yield. (H) MRC-5 cells were treated with cytarabine and infected with Ad-late/RFP as described above. Error bars represent SD (n = 2 for panels A and D; n = 3 for panels C and G).

fluctuations in the live-cell imaging chamber on cell health and virus growth; (ii) poor microscope focus for the detection and quantification of RFP due to presence of cell media (compared to PBS for the fixed-cell method); and (iii) 20–30 min time difference between reading the first and last wells of the 96-well screen plates, which can contribute to experimental differences. Consequently, we demonstrated that a fixed-cell screening method can be used to perform small molecule screens to identify novel HAdV inhibitors, as well as enhancers which can potentially be used to increase the expression level of therapeutic transgenes encoded within HAdV-based gene therapy vectors. Importantly, our screening procedure can be easily adapted for screening larger drug libraries in a high-throughput manner.

Using the screening platform we developed, we screened the Prestwick Chemical Library containing ~1200 chemically and pharmacologically diverse compounds (Fig. 2). Although we chose to use one cell line, a single compound concentration and a pretreatment strategy in this proof-of-concept study to test the functionality of the screen methodology, these conditions can be easily modified to discover compounds that impact different aspects of virus biology. For example, varying treatment strategies may allow the identification of positive hits that can

interfere at specific stages of an ongoing infection, while employing several compound concentrations and multiple cell lines (e.g. primary or transformed) could provide data on the general efficacy of the positive hits prior to further validation. One of the main advantages of the Prestwick library is that most of the compounds in it are FDA-approved, which could make the transitioning of positive hits from *in vitro* to *in vivo* models (and ultimately to humans) easier due to the availability of information on dosing, kinetics, bioavailability and safety. Of the eleven confirmed positive hits from the screen (Table 1), we conducted further assays on six (digoxin, digitoxigenin, lanatoside C, cytarabine, dexamethasone acetate and flunisolide) to characterize their impact on the virus lifecycle. Digoxin, digitoxigenin and lanatoside C are cardiac glycosides that function by inhibiting the activity of Na^+/K^+-ATPases (Fozzard and Sheets, 1985; Prassas and Diamandis, 2008). These compounds reduced Ad-late/RFP early/late gene expression, DNA replication and virus yield at nanomolar concentrations (Figs. 3 and 4), and the results are consistent with a previous report showing that cardiotonic steroids suppress HAdV replication (Grosso et al., 2017). The antiviral effects were not specific to A549 cells and the Ad-late/RFP, as late gene expression was decreased to a similar extent in MRC-5 cells, and for HAdV-4 and HAdV-7 (Fig. 4 and S1). It is possible that reduced viral DNA replication and late gene expression is a direct consequence of low E1A levels, as E1A is required for the transcriptional activation of the other viral genes (Berk, 1986). Differential splicing of the primary transcript produced from the E1A region gives rise to five different transcripts, of which, the 13S and 12S are the most abundant in early infection and the 9S is the major form in late infection (Stephens and Harlow, 1987). Grosso et al. found that cardiotonic steroids alter the localization of cellular SR proteins, leading to changes in viral early RNA splicing and in the relative levels of the transcripts such that the 13S increased in early infection and 12S increased in late infection, while 9S decreased to a similar extent at both times (Grosso et al., 2017). In our RT-qPCR experiments, we used primers which bind to cDNA generated from both the 13S and 12S RNAs. However, despite the marked decrease in overall E1A protein amount, we did not detect any obvious alterations in the expressed isoforms of E1A protein or the quantity of E1A transcripts (Fig. 4), suggesting that other mechanisms may also be involved. Cardiotonic steroids have shown antiviral activity against other DNA viruses (e.g. CMV and HSV) and in these cases, virus inhibition was due to impaired viral gene expression, protein translation and virus release (Amarelle and Lecuona, 2018; Cohen et al., 2016; Dodson et al., 2007; Su et al., 2008). Future studies should involve investigation of whether these mechanisms also play a role in the abrogation of HAdV by cardiotonic steroids.

Cytarabine, another positive hit from our screen, is a deoxycytidine analogue that interferes with DNA and RNA synthesis (Lamba, 2009). This chemotherapeutic agent has demonstrated antiviral activity against both DNA and RNA viruses (Hawley et al., 2013; Hryniuk et al., 1972), and is thought to act through the inhibition of viral DNA polymerases. Although we did not detect any obvious changes in viral DNA or RNA levels with cytarabine in our assays/time points, it indeed reduced late gene expression from Ad-late/RFP (in both transformed and primary cells) and virus yield at low concentrations (Figs. 3 and 5). Since higher plasma levels of cytarabine are frequently observed during treatment (Ersvaer et al., 2015; Momparler, 2013), higher concentrations of the drug may be used to obtain a more pronounced difference in HAdV yield, gene expression and nucleic acid synthesis. Infection of cells treated with glucocorticoid receptor agonists dexamethasone and flunisolide also reduced viral early/late proteins and yield (Fig. 5). These compounds modulate a multitude of cellular pathways and have an overall anti-inflammatory, immunosuppressive and anti-proliferative effects on cells (Almawi and Melemedjian, 2002). Thus, their anti-HAdV activity may be a consequence of their ability to alter cell signaling and homeostasis.

With digitoxigenin, cytarabine and the corticosteroids, we observed a lower impact on viral gene expression and replication at 48 hpi. Based on these results alone, we cannot conclude whether this is due to a complete but transient inhibition, which delays the onset of viral gene expression and replication, or whether the compounds allowed limited expression throughout infection, leading to a slow accumulation of viral transcripts/proteins/DNA at 48 hpi. We also note that the corticosteroids did not exhibit antiviral activity in MRC-5 cells, or against HAdV-4 and HAdV-7 (data not shown), which emphasizes the importance of validating positive hits from small molecule screens using multiple cell lines and virus types. However, further investigation of cytarabine, dexamethasone and flunisolide as anti-HAdV-5 agents is warranted since all three compounds displayed higher efficacy with lower MOIs of Ad-late/RFP (Fig. 5 and S2). In clinical settings, where infection generally occurs at low MOIs, these compounds may reduce virus replication sufficiently to allow host immune system a greater opportunity to combat the infection.

In conclusion, the small molecule screening platform we have developed has the required sensitivity to detect varying degrees of drug-induced changes in HAdV gene expression and replication, and therefore, can be used to efficiently conduct high-throughput screens to identify modulators of virus growth. This screening system permits the discovery of new HAdV inhibitors with different efficacies, including pre-existing drugs which have already been evaluated for *in vivo* safety and pharmacokinetics. Elucidating the mechanism by which these anti-HAdV compounds (e.g. the cardiotonic steroids, corticosteroids) exert their effects will not only enhance our knowledge of cellular pathways that play a role in HAdV lytic infection, but will also enable the identification of novel pharmacological targets and the development of more effective antivirals against HAdV.

Declarations of interest

None.

Acknowledgements

We thank Dr. Julien Yockell-Lelievre, Dr. Simon-Pierre Demers and Musfira Uvaize for assistance with protocol optimization for RFP imaging and quantification using the Cellomics ArrayScan platform and the HCS Studio software. We also thank Ms. Kathy Poulin for excellent technical assistance. This research was supported by grants to Dr. Robin Parks from the Canadian Institute of Health Research (CIHR) and the Natural Sciences and Engineering Research Council of Canada. Bratati Saha was supported by the Ontario Graduate Scholarship (OGS) and the Queen Elizabeth II Graduate Scholarship in Science and Technology from the Government of Ontario. Oliver Varette was supported by OGS and the Frederick Banting and Charles Best Canada Graduate Scholarship from CIHR. Infrastructure was supported by grants to Dr. William Stanford from the Canadian Foundation for Innovation and from the Province of Ontario. Dr. Jean-Simon Diallo was supported by a New Investigator Award in Infection and Immunity from CIHR.

Appendix A. Supplementary data

Supplementary data to this article can be found online at https://doi.org/10.1016/j.virol.2019.09.005.

References

Ahi, Y.S., Mittal, S.K., 2016. Components of adenovirus genome packaging. Front. Microbiol. 7, 1503.
Almawi, W.Y., Melemedjian, O.K., 2002. Molecular mechanisms of glucocorticoid antiproliferative effects: antagonism of transcription factor activity by glucocorticoid receptor. J. Leukoc. Biol. 71, 9–15.
Amarelle, L., Lecuona, E., 2018. The antiviral effects of Na,K-ATPase inhibition: a minireview. Int. J. Mol. Sci. 19, 2154.
Avgousti, D.C., Della Fera, A.N., Otter, C.J., Herrmann, C., Pancholi, N.J., Weitzman, M.D., 2017. Adenovirus core protein VII downregulates the DNA damage response on the host genome. J. Virol. 91 e01089-01017.
Berk, A.J., 1986. Adenovirus promoters and E1A transactivation. Annu. Rev. Genet. 20, 45–79.
Berk, A.J., 2007. Adenoviridae: the viruses and their replication. In: Knipe, D.M., Howley, P.M. (Eds.), Fields Virology, 5 ed. Lippincott Williams & Wilkins, Philadelphia, PA,

USA, pp. 2355–2394.
Bhatti, Z., Dhamoon, A., 2017. Fatal adenovirus infection in an immunocompetent host. Am. J. Emerg. Med. 35 1034.e1031-1034.e1032.
Binder, A.M., Biggs, H.M., Haynes, A.K., Chommanard, C., Lu, X., Erdman, D.D., Watson, J.T., Gerber, S.I., 2017. Human adenovirus surveillance - United States, 2003-2016. MMWR (Morb. Mortal. Wkly. Rep.) 66, 1039–1042.
Blackford, A.N., Grand, R.J.A., 2009. Adenovirus E1B 55-kilodalton protein: multiple roles in viral infection and cell transformation. J. Virol. 83, 4000–4012.
Caruso Brown, A.E., Cohen, M.N., Tong, S., Braverman, R.S., Rooney, J.F., Giller, R., Levin, M.J., 2015. Pharmacokinetics and safety of intravenous cidofovir for life-threatening viral infections in pediatric hematopoietic stem cell transplant recipients. Antimicrob. Agents Chemother. 59, 3718–3725.
Chartier, C., Degryse, E., Gantzer, M., Dieterle, A., Pavirani, A., Mehtali, M., 1996. Efficient generation of recombinant adenovirus vectors by homologous recombination in Escherichia coli. J. Virol. 70, 4805–4810.
ClinicalTrialsgov, Administration of Virus-specific Cytotoxic T-Lymphocytes (NCT00590083).
ClinicalTrialsgov, Clinical Grade Adenovirus Specific T Cells for Immunotherapy after Allogeneic Stem Cell Transplantation (NCT02851576).
Cohen, T., Williams, J.D., Opperman, T.J., Sanchez, R., Lurain, N.S., Tortorella, D., 2016. Convallatoxin-induced reduction of methionine import effectively inhibits human cytomegalovirus infection and replication. J. Virol. 90, 10715–10727.
de Jong, R.N., Meijer, L.A.T., van der Vliet, P.C., 2003. DNA binding properties of the adenovirus DNA replication priming protein pTP. Nucleic Acids Res. 31, 3274–3286.
de Wispelaere, M., Carocci, M., Liang, Y., Liu, Q., Sun, E., Vetter, M.L., Wang, J., Gray, N.S., Yang, P.L., 2017. Discovery of host-targeted covalent inhibitors of dengue virus. Antivir. Res. 139, 171–179.
Detweiler, C.J., Mueller, S.B., Sung, A.D., Saullo, J.L., Prasad, V.K., Cardona, D.M., 2018. Brincidofovir (CMX001) toxicity associated with epithelial apoptosis and crypt drop out in a hematopoietic cell transplant patient: challenges in distinguishing drug toxicity from GVHD. J. Pediatr. Hematol. Oncol. 40, e364–e368.
Dhingra, A., Hage, E., Ganzenmueller, T., Bottcher, S., Hofmann, J., Hamprecht, K., Obermeier, P., Rath, B., Hausmann, F., Dobner, T., Heim, A., 2019. Molecular evolution of human adenovirus (HAdV) species C. Sci. Rep. 9, 1039.
Dodson, A.W., Taylor, T.J., Knipe, D.M., Coen, D.M., 2007. Inhibitors of the sodium potassium ATPase that impair herpes simplex virus replication identified via a chemical screening approach. Virology 366, 340–348.
Doherty, J.E., Kane, J.J., 1973. Clinical pharmacology and therapeutics use of digitalis glycosides. Drugs 6, 182–221.
Duffy, M.R., Parker, A.L., Kalkman, E.R., White, K., Kovalskyy, D., Kelly, S.M., Baker, A.H., 2013. Identification of novel small molecule inhibitors of adenovirus gene transfer using a high throughput screening approach. J. Control. Release : Off. J. Control. Release. Soc. 170, 132–140.
Ersvaer, E., Brenner, A.K., Vetas, K., Reikvam, H., Bruserud, O., 2015. Effects of cytarabine on activation of human T cells - cytarabine has concentration-dependent effects that are modulated both by valproic acid and all-trans retinoic acid. BMC Pharmacol. Toxicol. 16, 12.
Ferrari, R., Pellegrini, M., Horwitz, G.A., Xie, W., Berk, A.J., Kurdistani, S.K., 2008. Epigenetic reprogramming by adenovirus e1a. Science 321, 1086–1088.
Flint, J., 1999. Adenoviruses: Basic Biology to Gene Therapy. Landes Company, pp. 17–30.
Fozzard, H.A., Sheets, M.F., 1985. Cellular mechanism of action of cardiac glycosides. J. Am. Coll. Cardiol. 5, 10a–15a.
Frisch, S.M., Mymryk, J.S., 2002. Adenovirus-5 E1A: paradox and paradigm. Nat. Rev. Mol. Cell Biol. 3, 441–452.
Grosso, F., Stoilov, P., Lingwood, C., Brown, M., Cochrane, A., 2017. Suppression of adenovirus replication by cardiotonic steroids. J. Virol. 91 e01623-16.
Hartline, C.B., Keith, K.A., Eagar, J., Harden, E.A., Bowlin, T.L., Prichard, M.N., 2018. A standardized approach to the evaluation of antivirals against DNA viruses: orthopox-, adeno-, and herpesviruses. Antivir. Res. 159, 104–112.
Hawley, T., Spear, M., Guo, J., Wu, Y., 2013. Inhibition of HIV replication in vitro by clinical immunosuppressants and chemotherapeutic agents. Cell Biosci. 3, 22.
Hilleman, M.R., Werner, J.H., 1954. Recovery of new agent from patients with acute respiratory illness. In: Proceedings of the Society for Experimental Biology and Medicine. Society for Experimental Biology and Medicine (New York, N.Y.), vol.85. pp. 183–188.
Horwitz, G.A., Zhang, K., McBrian, M.A., Grunstein, M., Kurdistani, S.K., Berk, A.J., 2008. Adenovirus small e1a alters global patterns of histone modification. Science 321, 1084–1085.
Horwitz, M.S., 2004. Function of adenovirus E3 proteins and their interactions with immunoregulatory cell proteins. J. Gene Med. 6 (Suppl. 1), S172–S183.
Hryniuk, W., Foerster, J., Shojania, M., Chow, A., 1972. Cytarabine for herpesvirus infections. J. Am. Med. Assoc. 219, 715–718.
Johansen, L.M., Brannan, J.M., Delos, S.E., Shoemaker, C.J., Stossel, A., Lear, C., Hoffstrom, B.G., Dewald, L.E., Schornberg, K.L., Scully, C., Lehár, J., Hensley, L.E., White, J.M., Olinger, G.G., 2013. FDA-approved selective estrogen receptor modulators inhibit Ebola virus infection. Sci. Transl. Med. 5, 190ra179.
Kajon, A.E., Ison, M.G., 2016. Severe infections with human adenovirus 7d in 2 adults in family, Illinois, USA, 2014. Emerg. Infect. Dis. J. 22, 730.
Keyes, A., Mathias, M., Boulad, F., Lee, Y.J., Marchetti, M.A., Scaradavou, A., Spitzer, B., Papanicolaou, G.A., Wieczorek, I., Busam, K.J., 2016. Cutaneous involvement of disseminated adenovirus infection in an allogeneic stem cell transplant recipient. Br. J. Dermatol. 174, 885–888.
King, C.R., Zhang, A., Tessier, T.M., Gameiro, S.F., Mymryk, J.S., 2018. Hacking the cell: network intrusion and exploitation by adenovirus E1A. mBio 9 e00390-00318.
Kojaoghlanian, T., Flomenberg, P., Horwitz, M.S., 2003. The impact of adenovirus infection on the immunocompromised host. Rev. Med. Virol. 13, 155–171.
Krokan, H., Wist, E., Krokan, R.H., 1981. Aphidicolin inhibits DNA synthesis by DNA polymerase alpha and isolated nuclei by a similar mechanism. Nucleic Acids Res. 9, 4709–4719.
Lamba, J.K., 2009. Genetic factors influencing cytarabine therapy. Pharmacogenomics 10, 1657–1674.
Lenaerts, L., De Clercq, E., Naesens, L., 2008. Clinical features and treatment of adenovirus infections. Rev. Med. Virol. 18, 357–374.
Lion, T., 2014. Adenovirus infections in immunocompetent and immunocompromised patients. Clin. Microbiol. Rev. 27, 441–462.
Luthra, P., Liang, J., Pietzsch, C.A., Khadka, S., Edwards, M.R., Wei, S., De, S., Posner, B., Bukreyev, A., Ready, J.M., Basler, C.F., 2018. A high throughput screen identifies benzoquinoline compounds as inhibitors of Ebola virus replication. Antivir. Res. 150, 193–201.
Marrugal-Lorenzo, J.A., Serna-Gallego, A., Gonzalez-Gonzalez, L., Bunuales, M., Poutou, J., Pachon, J., Gonzalez-Aparicio, M., Hernandez-Alcoceba, R., Sanchez-Cespedes, J., 2018. Inhibition of adenovirus infection by mifepristone. Antivir. Res. 159, 77–83.
Momparler, R.L., 2013. Optimization of cytarabine (ARA-C) therapy for acute myeloid leukemia. Exp. Hematol. Oncol. 2, 20.
Nun, T.K., Kroll, D.J., Oberlies, N.H., Soejarto, D.D., Case, R.J., Piskaut, P., Matainaho, T., Hilscher, C., Wang, L., Dittmer, D.P., Gao, S.-J., Damania, B., 2007. Development of a fluorescence-based assay to screen antiviral drugs against Kaposi's sarcoma associated herpesvirus. Mol. Cancer Ther. 6, 2360–2370.
Parker, E.J., Botting, C.H., Webster, A., Hay, R.T., 1998. Adenovirus DNA polymerase: domain organisation and interaction with preterminal protein. Nucleic Acids Res. 26, 1240–1247.
Pilger, B.D., Cui, C., Coen, D.M., 2004. Identification of a small molecule that inhibits herpes simplex virus DNA polymerase subunit interactions and viral replication. Chem. Biol. 11, 647–654.
Prassas, I., Diamandis, E.P., 2008. Novel therapeutic applications of cardiac glycosides. Nat. Rev. Drug Discov. 7, 926.
Ramsay, I.D., Attwood, C., Irish, D., Griffiths, P.D., Kyriakou, C., Lowe, D.M., 2017. Disseminated adenovirus infection after allogeneic stem cell transplant and the potential role of brincidofovir - case series and 10 year experience of management in an adult transplant cohort. J. Clin. Virol. : Off. Publ. Pan Am. Soc. Clin. Virol. 96, 73–79.
Reich, N.C., Sarnow, P., Duprey, E., Levine, A.J., 1983. Monoclonal antibodies which recognize native and denatured forms of the adenovirus DNA-binding protein. Virology 128, 480–484.
Ronchi, A., Doern, C., Brock, E., Pugni, L., Sanchez, P.J., 2014. Neonatal adenoviral infection: a seventeen year experience and review of the literature. J. Pediatr. 164, 529–535 e521-524.
Ross, P.J., Kennedy, M.A., Christou, C., Risco Quiroz, M., Poulin, K.L., Parks, R.J., 2011. Assembly of helper-dependent adenovirus DNA into chromatin promotes efficient gene expression. J. Virol. 85, 3950–3958.
Ross, P.J., Parks, R.J., 2009. Construction and characterization of adenovirus vectors. Cold Spring Harb. Protoc. 2009 (5), pdb.prot5011.
Rowe, W.P., Huebner, R.J., Gilmore, L.K., Parrott, R.H., Ward, T.G., 1953. Isolation of a cytopathogenic agent from human adenoids undergoing spontaneous degeneration in tissue culture. In: Proceedings of the Society for Experimental Biology and Medicine. Society for Experimental Biology and Medicine (New York, N.Y.), vol.84. pp. 570–573.
Saha, B., Parks, R.J., 2017. Human adenovirus type 5 vectors deleted of early region 1 (E1) undergo limited expression of early replicative E2 proteins and DNA replication in non-permissive cells. PLoS One 12, e0181012.
Saha, B., Parks, R.J., 2019. Histone deacetylase inhibitor suberoylanilide hydroxamic acid suppresses human adenovirus gene expression and replication. J. Virol. 93 e00088-19.
Saha, B., Wong, C.M., Parks, R.J., 2014. The adenovirus genome contributes to the structural stability of the virion. Viruses 6, 3563–3583.
Sanchez-Cespedes, J., Martinez-Aguado, P., Vega-Holm, M., Serna-Gallego, A., Candela, J.I., Marrugal-Lorenzo, J.A., Pachon, J., Iglesias-Guerra, F., Vega-Perez, J.M., 2016. New 4-Acyl-1-phenylaminocarbonyl-2-phenylpiperazine derivatives as potential inhibitors of adenovirus infection. Synthesis, biological evaluation, and structure-activity relationships. J. Med. Chem. 59, 5432–5448.
Sanchez-Cespedes, J., Moyer, C.L., Whitby, L.R., Boger, D.L., Nemerow, G.R., 2014. Inhibition of adenovirus replication by a trisubstituted piperazin-2-one derivative. Antivir. Res. 108, 65–73.
Stephens, C., Harlow, E., 1987. Differential splicing yields novel adenovirus 5 E1A mRNAs that encode 30 kd and 35 kd proteins. EMBO J. 6, 2027–2035.
Stray, S.J., Johnson, J.M., Kopek, B.G., Zlotnick, A., 2006. An in vitro fluorescence screen to identify antivirals that disrupt hepatitis B virus capsid assembly. Nat. Biotechnol. 24, 358–362.
Su, C.T., Hsu, J.T., Hsieh, H.P., Lin, P.H., Chen, T.C., Kao, C.L., Lee, C.N., Chang, S.Y., 2008. Anti-HSV activity of digitoxin and its possible mechanisms. Antivir. Res. 79, 62–70.
Thomas, G.P., Mathews, M.B., 1980. DNA replication and the early to late transition in adenovirus infection. Cell 22, 523–533.
Tollefson, A.E., Scaria, A., Hermiston, T.W., Ryerse, J.S., Wold, L.J., Wold, W.S., 1996. The adenovirus death protein (E3-11.6K) is required at very late stages of infection for efficient cell lysis and release of adenovirus from infected cells. J. Virol. 70, 2296–2306.
Wang, X., Zhang, Q., Zhou, Z., Liu, M., Chen, Y., Li, J., Xu, L., Guo, J., Li, Q., Yang, J., Wang, S., 2018. Retinoic acid receptor beta, a potential therapeutic target in the inhibition of adenovirus replication. Antivir. Res. 152, 84–93.
Weitzman, M.D., 2005. Functions of the adenovirus E4 proteins and their impact on viral vectors. Front. Biosci. : J. Vis. Lit. 10, 1106–1117.

Wodrich, H., Guan, T., Cingolani, G., Von Seggern, D., Nemerow, G., Gerace, L., 2003. Switch from capsid protein import to adenovirus assembly by cleavage of nuclear transport signals. EMBO J. 22, 6245–6255.
Wong, C.M., Poulin, K.L., Tong, G., Christou, C., Kennedy, M.A., Falls, T., Bell, J.C., Parks, R.J., 2016. Adenovirus-mediated expression of the p14 fusion-associated small transmembrane protein promotes cancer cell fusion and apoptosis in vitro but does not provide therapeutic efficacy in a xenograft mouse model of cancer. PLoS One 11 e0151516-e0151516.
Ying, B., Tollefson, A.E., Spencer, J.F., Balakrishnan, L., Dewhurst, S., Capella, C., Buller, R.M., Toth, K., Wold, W.S., 2014. Ganciclovir inhibits human adenovirus replication and pathogenicity in permissive immunosuppressed Syrian hamsters. Antimicrob. Agents Chemother. 58, 7171–7181.
Young, C.S., 2003. The structure and function of the adenovirus major late promoter. Curr. Top. Microbiol. Immunol. 272, 213–249.
Zhao, H., Granberg, F., Elfineh, L., Pettersson, U., Svensson, C., 2003. Strategic attack on host cell gene expression during adenovirus infection. J. Virol. 77, 11006–11015.